View metadata, citation and similar papers at core.ac.uk
brought to you by CORE
provided by Lancaster E-Prints

The interplay between transport and reaction rates as controls on nitrate attenuation in permeable, streambed sediments.

Author list:

K. Lansdown[1,2], C.M. Heppell[1*], M. Trimmer[2], A. Binley[3], A.L. Heathwaite[3], P. Byrne[3†] and H. Zhang[3]

Affiliations:

[1] School of Geography, Queen Mary, University of London, Mile End Road, London E1 4NS, England

[2] School of Biological and Chemical Sciences, Queen Mary, University of London, Mile End Road, London E1 4NS, England

[3] Lancaster Environment Centre, Lancaster University, Lancaster LA1 4YQ

*Corresponding author: c.m.heppell@qmul.ac.uk

[†]Current address: School of Natural Sciences and Psychology, Liverpool John Moores University, Liverpool L3 3AF

Submitted to:

JGR Biogeosciences

Key points:

1. Deep sediments (>10cm) are nitrate sinks in groundwater-fed rivers
2. Denitrification can be sustained without substantial buried organic matter
3. Denitrification in a sand-dominated reach can be transport-controlled.

Abstract:

Anthropogenic nitrogen fixation and subsequent use of this nitrogen as fertilizer has greatly disturbed the global nitrogen cycle. Rivers are recognized hotspots of nitrogen removal in the landscape as interaction between surface water and sediments creates heterogeneous redox environments conducive for nitrogen transformations. Our understanding of riverbed nitrogen dynamics to date comes mainly from shallow sediments or hyporheic exchange flow pathways with comparatively little attention paid to groundwater-fed, gaining reaches. We have used ^{15}N techniques to quantify in situ rates of nitrate removal to 1m depth within a groundwater-fed riverbed where subsurface hydrology ranged from strong upwelling to predominantly horizontal water fluxes. We combine these rates with detailed hydrologic measurements to investigate the interplay between biogeochemical activity and water transport in controlling nitrogen attenuation along upwelling flow pathways. Nitrate attenuation occurred via denitrification rather than dissimilatory nitrate reduction to ammonium or anammox (range = 12 to >17000 nmol $^{15}N\ L^{-1}\ h^{-1}$). Overall, nitrate removal within the upwelling groundwater was controlled by water flux rather than reaction rate (i.e. Damköhler numbers < 1) with the exception of two hotspots of biogeochemical activity. Deep sediments were as important a nitrate sink as shallow sediments with fast rates of denitrification and short water residence time close to the riverbed surface balanced by slower rates of denitrification and water flux at depth. Within this permeable riverbed >80% of nitrate removal occurs within sediments not exposed to hyporheic exchange flows under baseflow conditions, illustrating the importance of deep sediments as nitrate sinks in upwelling systems.

Key words: (up to 6 keywords) hyporheic, nitrate consumption, hot spots, denitrification, residence time, Damköhler

1 Introduction

The global challenge of nitrate saturation of freshwater environments arises from increased nitrogen loading to rivers due to anthropogenic activities such as land use change, domestic and industrial wastewater treatment and intensification of agricultural practice [*Bernot and Dodds*, 2005; *Caraco and Cole*, 1999]. In the United Kingdom, nitrate concentrations in many rivers and groundwaters have increased since the 1970s [*Burt et al.*, 2011] leading to coastal eutrophication [*Maier et al.*, 2009], and increasing the costs of drinking water supply in order to meet standards designed to protect the environment [*Knapp*, 2005; *National Audit Office*, 2010]. Monitoring data for regulatory purposes indicates that whilst nitrate concentrations in many UK rivers have now plateaued, that concentrations in groundwater-fed rivers continue to rise [*Burt et al.*, 2011; *Howden and Burt*, 2008]. This nitrate legacy has renewed interest in the role that naturally occurring microbially-mediated processes might play in transforming (e.g. dissimilatory nitrate reduction to ammonium) and removing (in the case of denitrification and anaerobic ammonium oxidation, anammox) nitrate in riverbeds [*Rivett et al.*, 2008; *Stelzer and Bartsch*, 2012].

Considerable attention has been placed on the potential role of the hyporheic zone for nitrate removal from surface waters via denitrification [*Smith*, 2005], and on hyporheic exchange flows (HEFs) as a means of delivering nitrate-rich surface water to the stream bed where microbial activity and denitrification rates are enhanced [*Findlay et al.*, 2003; *Fischer et al.*, 2005]. Problems of nitrate enrichment are particularly pertinent, however, for groundwater-fed rivers in permeable catchments with high N-loading rates where nitrate-rich groundwater will dominate baseflow. The need to understand nitrogen transformations in gaining river settings have led to an alternative 'bottom-up' rather than 'top-down' conceptualization of nitrate removal processes, highlighting the importance of measuring nitrogen transformations in deep stream sediments [*Stelzer and Bartsch*, 2012]. Many experimental studies of nitrogen cycling in stream riverbeds focus on the upper 10cm of the riverbed often selecting to conduct experiments *ex situ* by physically removing sediments,

77 which changes the redox environment and supply of reactants making investigation of the complete
78 nitrogen cycle impossible [*Addy et al.*, 2002; *Sheibley et al.*, 2003]. Likewise, where field studies of
79 nitrogen transformations are attempted, the general approach has been to focus on 'soft' riverbeds
80 sediments due to the logistical difficulties associated with working within armored gravel or cobble-
81 sized material [*Stelzer et al.*, 2011]. To advance our understanding it is critical that we measure *in*
82 *situ* rates of denitrification along with other components of the nitrogen cycle (such as nitrification,
83 anammox and N_2O production), at depths greater than 10cm in the coarse-grained sediments typical
84 of groundwater-fed systems, so that the relative importance of denitrification in comparison with
85 other nitrate removal processes can be fully evaluated. Application of ^{15}N-labelled substrates is the
86 only method by which multiple pathways of nitrogen cycling can be investigated directly and
87 simultaneously. Injection of $^{15}NO_3^-$ into saturated sediments and recovery of porewaters over time
88 [referred to as 'push-pull' sampling; *Istok et al.*, 1997] has been performed at depth within the
89 riverbed and also through groundwater monitoring wells [*Addy et al.*, 2002; *Clilverd et al.*, 2008].
90 These measurements, however, were focused on quantifying denitrification within large volumes of
91 sediment (10-20L of tracer were injected) and, consequently, had quite wide vertical resolution (e.g.
92 30-60cm). Finer scale ^{15}N 'push-pull' investigations have also been performed [*Burgin and*
93 *Hamilton*, 2008; *Lansdown et al.*, 2014; *Sanders and Trimmer*, 2006], but to date, not in
94 conjunction with detailed hydrologic measurements.
95
96 The extent to which nitrate is exported from groundwater to surface waters in an upwelling
97 groundwater setting will be controlled by the rate of biogeochemical nitrate removal and the flux of
98 water through the riverbed. The Damköhler number, a dimensionless ratio of reaction rate to
99 transport rate of the solute, can be used to contrast the importance of these two drivers of nitrate
100 removal [*Gu et al.*, 2007; *Ocampo et al.*, 2006]. Damköhler numbers have been widely used in
101 contaminant studies in the hydrogeological literature [*Bahr and Rubin*, 1987] and have also been
102 applied to denitrification in hyporheic zones to distinguish between hydrological and

103 biogeochemical controls on nitrate removal from thalweg and marginal sediments [*Harvey et al.*,
104 2013]. Recent modelling studies have focused on using residence time analysis to distinguish
105 between zones of net nitrification and denitrification along hyporheic flow pathways [*Bardini et al.*,
106 2012; *Marzadri et al.*, 2011; *Zarnetske et al.*, 2012]. Other processes of nitrate reduction, such as
107 anammox have largely been ignored because their role in nitrate removal is currently thought by
108 many researchers to be negligible [*Burgin and Hamilton*, 2007].
109
110 *Stelzer* and *Bartsch* [2012] have recently developed a conceptual model of nitrate-rich gaining
111 fluvial settings in which nitrate-rich oxic groundwater upwells through deeper riverbed sediments to
112 reach a zone enriched with electron donors in the form of particulate organic matter from surface
113 waters. This organically-enriched layer, arising from the deposition and burial of particulate organic
114 matter and varying in thickness (dependent on deposition rate, vertical hydraulic gradient and
115 porosity), facilitates the development of hypoxic and anoxic conditions to drive nitrate reduction
116 processes such as denitrification. To date this 'bottom-up' conceptualization of gaining reach
117 settings has focused on the interaction of upwelling groundwater with shallow hyporheic exchange
118 flows (HEF). Here, we develop the conceptual model further to evaluate the effect of deeper
119 (> 10cm depth) horizontal subsurface flows on nitrate reduction processes.
120
121 We have previously used measurements of saturated hydraulic conductivity with vertical head
122 gradient from a network of piezometers in a gaining, permeable sandstone reach to show that even
123 in a strongly upwelling stream horizontal water fluxes (both lateral and longitudinal; Figure 1a) can
124 influence of on hyporheic zone chemistry [*Heppell et al.*, 2013]. By combining measurement of
125 water flux with an understanding of the spatial variability in redox patterns in the reach we could
126 distinguish nitrate-rich oxic conditions associated with upwelling groundwater from nitrate-poor
127 reducing conditions associated with horizontal flows from hyporheic exchange and/or riparian
128 flows [*Heppell et al.*, 2013]. We did not observe nitrate poor, reducing conditions associated with

129 strong groundwater upwelling, probably because the regional aquifer contains little organic carbon
130 [*Smith and Lerner*, 2008] and, as a result, is oxygenated [*Lapworth et al.*, 2008]. Here, we combine
131 our 3D measurements of spatial variability in vertical and horizontal hydrological fluxes (at a
132 spatial resolution not previously captured in gaining stream settings) with *in situ* process based
133 measurements of nitrate transformations to investigate the interplay between hydrological and
134 biogeochemical controls on nitrate consumption at the reach scale. We apply the use of Damköhler
135 numbers in order to distinguish between residence time and biogeochemical controls on nitrate
136 reduction in the stream sediments of our gaining reach.
137
138 Specifically, we:
139 (i) identify the spatial variability in nitrate consumption in a single gaining reach, focusing
140 on the depth distribution of nitrate attenuation.
141 (ii) investigate the factors that controls nitrate consumption in the reach, using Damköhler
142 numbers to explore the interplay between residence time (hydrological) and biogeochemical
143 controls on nitrate consumption.
144 (iii) estimate total nitrate consumption within the riverbed using our *in situ* hydrological and
145 biogeochemical measurements to quantify the significance of nitrate removal in deep (> 10
146 cm) bed sediments of a gaining reach.
147
148 **2 Methods**
149 2.1 Site description
150 Our 200m study site, located within the River Leith (Cumbria, UK), receives groundwater from the
151 Aeolian Penrith Sandstone, a major aquifer of the Permo-Triassic Sandstone in the UK [*Allen et al.*,
152 1997; *Seymour et al.*, 2008]. The gaining reach comprises sandstone bedrock overlain by
153 unconsolidated glacio-fluvial sands and silts (1-2 m) which are topped by sand, gravel and cobbles
154 forming riffle and pool sequences. The catchment of the River Leith is a mixed agricultural

155 landscape, and the river is a designated Site of Special Scientific Interest (SSSI) and Special Area of
156 Conservation (SAC).
157
158 2.2 Field sampling campaign
159 Riparian and in-stream piezometers (internal diameter = 27mm) were installed in clusters at the site
160 in June 2009 and June 2010 using a percussion drill (*see Binley et al.* [2013] for a detailed
161 description). Each in-stream cluster comprised three piezometers screened at 100cm, 50cm and
162 20cm depth to measure saturated hydraulic conductivity and head gradient. The 100cm in-stream
163 piezometers were fitted with multi-level porewater samplers at target depths of 10, 20, 30, 50 and
164 100cm in order to establish porewater chemistry and to enable tracers to be introduced at various
165 depths beneath the riverbed surface. The end of each porewater sampler was wrapped in a fine
166 polyester mesh to prevent ingress of sediment. Collection of porewater samples (total n=72), ^{15}N
167 injections into the multi-level porewater samplers and measurement of vertical hydraulic gradient
168 was performed at 9 points along the study reach (labelled A-I in Figure 1b) from 9-13 August, 2011
169 under low flow conditions (<0.5m^3 s^{-1}). At positions A, C and G a transect of three piezometer
170 clusters were examined (total number of piezometer clusters = 15) and we were unable to collect
171 porewater from three sampling tubes (G-20cm, H-30cm and I-50cm).
172
173 2.2.1 Porewater sampling
174 Prior to the injection of ^{15}N-NO_3^- (*see* below), a 40mL porewater sample was collected from each of
175 the multi-level samplers via a syringe. A sample of surface water was also collected at each
176 piezometer cluster. Samples for analysis of chloride and nitrogen species were filtered (0.2µm
177 polypropylene membrane, VWR International, UK) into plastic vials (polypropylene) in the field
178 and frozen until later chemical analysis (*see* below). Samples for analysis of dissolved organic
179 carbon (DOC) were filtered into acid-washed amber glass bottles and acidified to pH<2 with HCl in
180 the field. For determination of reduced iron (Fe(II)), 1 mL of water was filtered through an oxygen

181 free nitrogen-flushed 0.2µm filter (as above) into 4 mL of phenanthroline-acetate buffer solution
182 and stored in the dark until analysis by UV-spectrophotometry [*APHA-AWWA-WPCF*, 1976; *Grace*
183 *et al.*, 2010]. Water samples were also collected to determine the natural abundance ^{15}N content of
184 nitrogen gas (N_2) and dissolved nitrous oxide (N_2O) and methane concentrations. Gas tight vials
185 (Exetainer, Labco) were overflowed at least two times by gentle discharge of water through a 21-
186 gauge needle to minimize atmospheric exchange and bacterial activity was inhibited by addition of
187 zinc chloride (25µL, 7M). Dissolved oxygen (O_2) concentration was measured in the field using a
188 calibrated, fast response electrode (50µm, Unisense, Denmark). Water temperature and pH were
189 measured (pH-100 meter, VWR International, UK) following O_2 determination. For these
190 measurements, water was gently transferred via a three-way stop cock from the collection syringe
191 into an open syringe barrel containing the O_2 electrode or pH probe. We determined the amount of
192 O_2 contamination that occurred during sample transfer to be approximately 10 μM, and corrected all
193 measured O_2 concentrations accordingly.
194
195 2.2.2 *In situ* measurement of riverbed nitrate reduction
196 ^{15}N-labelled NO_3^- tracer (98 atom % ^{15}N, Sigma Aldrich) solution was prepared in the laboratory at
197 approximately the same concentration as ambient $^{14}NO_3^-$ (100, 200, 300, 400 or 500µM $^{15}NO_3^-$) and
198 de-oxygenated by bubbling with oxygen-free nitrogen gas (British Oxygen Company). The tracer
199 matrix was artificial river water [*Smart and Barko*, 1985] tailored to match the major ion chemistry
200 of the River Leith but with added chloride (~4mM KCl) to measure advective flow [*Lansdown et*
201 *al.*, 2014]. In the field, tracer was drawn into luer-lock syringes under oxygen-free nitrogen or after
202 sparging with air to match ambient O_2 conditions. Sub-samples of the tracer (*n*=3 per piezometer
203 cluster) were reserved for later chemical analysis and physico-chemical measurements (as above
204 and *see* below). 50mL of ^{15}N-NO_3^- tracer was injected into the riverbed via each multi-level
205 sampler, with all injections at a piezometer completed within 2.5h. Porewater samples (*n*=4, 7mL)
206 were collected over time after the dead volume of the sampling tube had been discarded. The first

207 porewater sample was recovered immediately after injection. Recovery of porewaters thereafter
208 occurred according to depth with collection of porewater from10 and 20cm samplers at 5, 10 and 30
209 minutes post injection; 30 and 50cm samplers at 10, 30 and 60 minutes post injection and 100cm
210 samplers at 15, 45 and 120 minutes post injection. Recovered porewater samples were split between
211 gas-tight vials for N_2 analysis and filtered into plastic tubes for anion analysis (using above
212 sampling procedures and analysis methods described below).
213
214 We worked from downstream to upstream, and from shallow to deep samplers, to ensure that there
215 was no cross-contamination of tracer plumes. Water flux was also sufficiently slow to prevent
216 mixing of tracer injected at different depths within the experimental time frame (*see* Results).
217 Assuming that the injection of the tracer forms a sphere centered at the terminus of the multi-level
218 sampler tube, the magnitude of the $^{15}NO_3^-$ dilution immediately post injection corresponds to a
219 sediment volume of 120 cm^3 (porosity = 0.35). Accordingly, each of our denitrification
220 measurements has a vertical resolution of approximately ± 3.2 cm.
221
222 2.2.3 Hydrological and sediment analyses
223 Sediment samples, collected from each core during piezometer installation, were divided into 10cm
224 increments in the field. On return to the laboratory, the sediment samples were air dried and divided
225 for loss on ignition (LOI) and granulometric analysis by sieving and laser diffraction. The < 1mm
226 fraction was digested with 30% hydrogen peroxide to remove organic matter and the samples was
227 dispersed in Calgon before particle size analysis with a Malvern 2000 Mastersizer, Malvern
228 Instruments Ltd., UK). Data from all size distributions were then combined to calculate d_{50} (mm).
229
230 Saturated hydraulic conductivity was measured using falling and rising slug tests in the piezometers
231 at 100, 50 and 20cm depth (*see Binley et al.,* [2013] for detailed description). Head levels in the in-
232 stream and bank piezometers were measured concurrently with push-pull measurements using an

electronic dip meter. Darcian vertical water flux (m d^{-1}) at 100, 50 and 20cm depth was calculated following the method described in *Binley et al.,* [2013], assuming permeability is isotropic.

2.3 Laboratory analyses

2.3.1 Porewater analysis

Nitrate (Limit of detection (LOD) 12 µM, precision 3%) and chloride (LOD 2 µM, precision 1%) were determined using ion exchange chromatography (Dionex ICS2500) whilst ammonium and nitrite were determined by automated colorimetric analysis (Skalar San++) with detection limits and precision of 0.3 µM ± 5% and 0.05 µM ± 1%, respectively. DOC was analyzed by the non-purgeable organic carbon method (Thermo TOC analyzer; LOD 23µM, precision 5%). N_2O and methane were determined using gas chromatography (Agilent Technologies) with electron capture and flame ionization detection, respectively, following addition of a helium headspace (*see* below).

2.3.2 Calculating *in situ* rates of nitrate reduction

A 500µL helium headspace was introduced to each 3mL gas-tight vial and equilibrated with the porewater overnight at 22°C. The ^{15}N-N_2 content was quantified using mass-to-charge ratios of 28, 29 and 30 measured with a mass spectrometer (Finnigan MAT DeltaPlus) calibrated and corrected for drift following the procedure described in *Trimmer et al.* [2006]. Precision as a coefficient of variation was better than 1%. Production of $^{29}N_2$ or $^{30}N_2$ was quantified as excess above natural abundance, adapted from *Thamdrup and Dalsgaard* [2000]:

$$\Delta N_{2\ t=i}\ (\text{nM}\ N_2) = \left[\left(\frac{^{x}N_2}{\Sigma N_2} \right)_{t=i} - \left(\frac{^{x}N_2}{\Sigma N_2} \right)_{\text{background}} \right] \text{x}\ \Sigma N_2\ \text{sample x}\ \alpha^{-1}\ \text{x}\ V_s^{-1} \qquad (1)$$

where $\Delta^x N_2$ is the amount of excess $^{29}N_2$ or $^{30}N_2$ in the recovered porewater at time=i; $^xN_2/\ \Sigma N_2$ represents the ratio of the $^{29}N_2$ or $^{30}N_2$ mass spectrometer signal to the total N_2 signal ($\Sigma N_2 = {}^{28}N_2 + {}^{29}N_2 + {}^{30}N_2$) for either time series or background samples; α is the calibration factor (signal: nmol N_2 $vial^{-1}$); and V_s is the volume of porewater in the gas-tight vial (L $vial^{-1}$). 'Excess' concentrations

258 of $^{29}N_2$ and $^{30}N_2$ in the tracer solution were also calculated via Eq. 1 (where t=i is the tracer) to
259 allow correction for loss through advective flow as follows:

260 $$\Delta'^{x}N_{2\ t=i}\ (\mathrm{nM}\ N_2) = \Delta^{x}N_{2\ t=i} + \left[\left(\frac{\left[Cl^-\right]_{t=i} - \left[Cl^-\right]_{tracer}}{\left[Cl^-\right]_{background} - \left[Cl^-\right]_{tracer}}\right) \mathrm{x}\ \Delta^{x}N_{2\ tracer}\right] \quad (2)$$

261 where: $\Delta'^{x}N_2$ is the concentration of $^{29}N_2$ or $^{30}N_2$ at time=i corrected for the loss of $^{15}NO_3^-$ tracer or
262 ^{15}N labelled products via advective flow; $\Delta^{x}N_{2\ t=i}$ and $\Delta^{x}N_2$ tracer are the excess of concentration
263 of $^{29}N_2$ or $^{30}N_2$ calculated from Eq. 1 in the time series samples and tracer solution, respectively;
264 and $[Cl^-]$ is the concentration of chloride in the tracer solution (tracer), ambient porewater
265 (background), and porewater collected over time following the injection of $^{15}NO_3^-$ (t=i).
266
267 The rate of $^{29}N_2$ and $^{30}N_2$ production ($p^{29}N_2$ or $p^{30}N_2$) was calculated by linear regression of
268 $\Delta'^{x}N_2$ t=i against time. The rate of denitrification was calculated according to *Nielsen* [1992]:

269 $$\text{Denitrification (nmol } {}^{15}\text{N-N}_2\ \text{L}^{-1}\ \text{h}^{-1}) = p^{29}N_2 + 2\ \mathrm{x}\ p^{30}N_2 \quad (3)$$

270 Note, as the ^{15}N-labelling of the N_2 and N_2O produced after injection of $^{15}NO_3^-$ was the same (*see*
271 Results) then the contribution of anammox to the production of N_2 gas could be assumed to be
272 negligible [*Trimmer et al.*, 2006] and, as a consequence, Nielsen's original formulation for the
273 isotope pairing technique remained perfectly valid [*Risgaard-Petersen et al.*, 2003].
274
275 The ^{15}N-labelling of the N_2O pool following injection of $^{15}NO_3^-$ was determined on a subset of
276 samples (n=49). To quantify ^{15}N-N_2O a 100µL sub-sample of the headspace of the gas-tight vial
277 (from above) was injected into an air-filled 12mL gas-tight vial (Exetainer, Labco). The entire
278 content of the gas-tight vial was swept, using a two-way needle and analytical grade helium, to a
279 trace gas preconcentrator (Cryo-Focusing; PreCon, Thermo-Finnigan), where the gases are dried
280 and cryo-focused twice in liquid N_2 and before final separation of N_2O from CO_2 on a PoraPLOT Q
281 capillary column. The sample then passes to mass spectrometer (as above) and the mass-to-charge
282 ratios of 44, 45 and 46 are measured. The amount of dissolved ^{15}N-N_2O was calculated by

283 multiplying the total concentration of N_2O, as measured by gas chromatography, by the proportion
284 of ^{15}N-label in the N_2O pool as determined by mass spectrometry (mass-to-charge = 45 / 2 x mass-
285 to-charge = 46). Concentrations of ^{15}N-N_2O were corrected for losses due to advective flow as per
286 equation 2, substituting N_2O for N_2 values. Rates of ^{15}N-N_2O production were then calculated by
287 linear regression of the corrected concentrations against time.
288
289 2.5 Data analyses
290 2.5.1 Assigning piezometer clusters to hydrologic setting using porewater chemistry.
291 Each piezometer cluster was assigned to one of three hydrologic settings using chloride
292 concentrations in a two end-member mixing model as follows:

293 $$\text{Mixing score} = \frac{\left[Cl^-\right]_{\text{porewater}} - \left[Cl^-\right]_{\text{surface water}}}{\left[Cl^-\right]_{\text{surface water}} - \left[Cl^-\right]_{\text{100cm}}} \quad (4)$$

294 where “porewater” refers to samples collected between 10 and 50cm depth in the riverbed and
295 “100cm” was porewater recovered from 100cm. Scores can range from -1 to 0. The lower range
296 indicates dominance of upwelling porewater and the higher range indicates maximum surface water
297 influence. Hydrology at piezometer was classed as strong porewater upwelling when scores were -1
298 and hyporheic exchange flows (HEF) when scores vary between -1 and 0. Horizontal water fluxes,
299 for example longitudinal flow along the river channel or lateral inputs from the riparian zone, were
300 inferred when scores were <-1 (no scores were >0). As such, horizontal water fluxes cannot be
301 detected with this method if chloride concentrations of the horizontal source are the same as surface
302 water and upwelling porewater. We are confident however, that the assigned hydrologic settings
303 reflect actual subsurface hydrology as classifications compare favorably with the zones of
304 upwelling, HEF and horizontal fluxes inferred through *in situ* measurements by *Binley et al.* [2013].
305
306 2.5.2 Calculations for integrating flux and nitrate removal in sediment via denitrification.

307 Initially, we examined the relative importance of denitrification activity at different depths in the
308 riverbed by simply contrasting rates of reaction, as per *Stelzer et al*. [2012; 2011]. The proportion of
309 denitrification activity at each depth was determined by dividing the individual rate by the sum of
310 all rates within a piezometer cluster (Table 1). We refer to these data as rate-determined
311 proportions.
312
313 Nitrate removal within a riverbed will depend not only upon the denitrification rate (as above) but
314 also on amount of time a parcel of water is exposed to a given denitrification rate (as per *Harvey et*
315 *al.* [2013]). In order to explore the effects of spatial variations in upwelling water flux on the extent
316 of nitrate removal via denitrification we calculated the residence time of upwelling water in each
317 sediment section (0-10cm, 10-20cm etc.) where residence time was the inverse of the relevant
318 Darcy vertical water flux. We measured saturated hydraulic conductivity at 20, 50 and 100 cm
319 depths only, so we estimated residence time of the 0-10cm and 30-50cm depth bands by assuming
320 vertical flux at 10cm was equal to vertical flux at 20cm and the vertical flux at 30cm was the
321 average of fluxes at 20 and 50cm. We then multiplied the *in situ* rate of denitrification (nmol $^{15}N\text{-}N_2$
322 $L^{-1}\ h^{-1}$) by the residence time (h) to calculate the amount of nitrate removed from each sediment
323 section as upwelling water passed through it. In order to express this nitrate removal on a sediment
324 volume basis (mmol N m^{-3}) we assumed a sediment porosity of 0.35 (-). Relative magnitudes of
325 denitrification activity within each sediment section were calculated as above, however, we refer to
326 these data as depth-integrated proportions.
327
328 Areal rates of denitrification (μmol N $m^{-2}\ h^{-1}$) were estimated by converting measured
329 denitrification rates (per volume of porewater) through integration of denitrification activity within
330 depth profiles (*see Laverman et al.* [2007] for similar calculations). Integration was performed
331 using the trapezium rule and the *in situ* denitrification rate in the 0-10cm depth band was estimated

by extrapolating the trend from measurements at 30, 20 and 10 cm data from shallow sediments to 0cm depth.

2.5.3 Damköhler number calculation

The Damköhler number for denitrification (Da_N) is the dimensionless ratio between a transport (τ_T) and denitrification reaction (τ_R) timescale. τ_T is the residence time (units = d) and τ_R is the inverse of the first-order reaction rate constant for denitrification, K_1 ($\tau_R = 1/K_1$, units for K_1 and τ_R are d^{-1} and d, respectively) [*Harvey et al.*, 2013]. Our denitrification rates were zero-order, i.e. production of ^{15}N-labelled N_2 was linear with time. To convert our data to first order rate constants we divided the zero-order rate constants (units = nmol L^{-1} h^{-1}) by the mean half saturation constant for denitrification (K_m = 109 μM) in rivers of north east England reported by García-Ruiz *et al.* [1998]. Da_N (τ_T / τ_R) values < 1 indicate that transport dominates over reaction, whilst values > 1 indicate that reaction processes are occurring faster than advection [*Ocampo et al.*, 2006].

2.5.4 Statistical analysis

All statistics were performed in R [*R Development Core Team*, 2012]. Differences in chemical parameters across sediment depth bands and hydrologic settings were investigated by two-way analysis of variance (ANOVA). Prior to each ANOVA we tested whether the data were normally distributed with a Shapiro Wilk test and attempted to normalize any data where $p>0.05$. For most variables however, distributions were unable to be normalized using common methods (e.g. log and power transformations) so we rank transformed data prior to the ANOVA. Any significant effects detected in the ANOVA ($p>0.05$) were further examined by pairwise comparisons using a Post-hoc Tukey's test. A paired t-test was used to test for any difference in the ^{15}N labelling of the N_2 and N_2O pools following $^{15}NO_3^-$ addition. Relationships between denitrification rate and chemical variables were explored using Spearman's rank correlation.

358 **3 Results**

359

360 **3.1 Summary of reach characteristics**

361 *General description of stratigraphy*

362 Median grain size (d_{50}) decreased with depth in the riverbed (Table 2); superficial sediments are a
363 mixture of coarse sand, gravel and small cobbles, whilst deep (> 10 cm) sediments are mainly sand.
364 Sediment particulate organic matter content was low, ranging from 0.3-3.3% (loss on ignition), and
365 decayed with depth (ANOVA, $F(4,33)=5.6$, $p=0.002$).

366

367 *Spatial distribution of porewater chemistry and water fluxes*

368 Vertical head gradients were positive throughout the ^{15}N injections period (range = 0.5 to 28%)
369 indicating upward movement of water from the sediments towards the river. Chloride profiles
370 provided further evidence of porewater upwelling but also revealed localized zones of surface water
371 downwelling and horizontal flows (e.g. plots B, F and D, respectively; Figure 1c). We examined
372 these water fluxes further using a two end-member mixing model, not to apportion water source in
373 the riverbed, as depth profiles suggested at least three sources of water were present at some sites,
374 but to quantitatively assign piezometer clusters to hydrologic settings. Subsurface hydrology could
375 be described as either strong porewater upwelling, surface water downwelling to ≤20cm (HEF) or
376 horizontal flows (n = 6, 5 and 4 respectively; Figure 2). Water residence time, based on a calculated
377 Darcy flux, varied from 0.11d to 32d for 10cm and 50cm flow pathways, respectively when water
378 flux was predominantly vertical (i.e. strong upwelling and/or HEF). Water residence times were
379 slightly longer when upwelling was strong (mean ± s.d. = 5±2d and 3±1d for upwelling and HEF,
380 respectively) and in deep sediments (mean ± s.d. = 0.7±0.1d and 2.2±0.5d per 10cm for sediments
381 from 0-20cm and 30-100cm, respectively).

382

383 Porewater nitrate concentrations were highly variable, ranging from below detection to ≥ 600μM at
384 each of the depths examined. Overall, nitrate concentrations within deep sediments (100cm) were
385 higher than those in the river (mean ± s.d. = 311±182 μM and 129±18 μM, respectively) and tended
386 to decrease towards the riverbed surface (Table 2). This trend was not statistically significant.
387 Along-reach variation in porewater nitrate was also evident (Figure 3a), and concentrations were
388 typically high in areas characterized by upwelling porewater (Figure 3b; $F(2,56)=11.1$, $p<0.001$).
389
390 Porewater DOC concentrations did not differ with depth in the riverbed (Table 2) relative to
391 variation across the study reach (Figure 3c). Shallow sediments at 10 cm depth exposed to HEF
392 were sites of elevated DOC (*see* points A, F and H in Figure 3c and DOC concentrations
393 summarized by depth and hydrology in Supplementary Information), although when integrating
394 data across all depths (0-100 cm), differences between hydrologic settings were not significant
395 (Figure 3d).
396
397 Porewaters were generally under-saturated in O_2 (mean ± s.d. = 49±21 %) and, like nitrate, oxygen
398 concentrations decreased towards the riverbed surface (Table 2, Figure 3e); although the trend was
399 not statistically significant. When considering depth-distributions, dissolved oxygen concentrations
400 were most heterogeneous at 10 cm depth in shallow sediments exposed to HEF (range = 308μM, 17
401 to 325μM). The next largest range in O_2 concentrations was 180μM (57 to 237 μM) at 50cm under
402 horizontal water flux. Highest median O_2 concentrations were associated with sediments dominated
403 by porewater upwelling (Figure 3f; ANOVA, $F(2,57)=6.9$, $p=0.002$), and these sediments were also
404 associated with the lowest concentrations of other reduced chemical species such as Fe(II) and
405 methane. Ammonium concentrations were highly variable both with depth in the riverbed and
406 across the reach, ranging from below detection to 125μM (mean ± s.d. = 5±19μM).
407
408 **3.2 Factors controlling *in situ* rates of denitrification and overall nitrate removal**

Quantification of in situ denitrification rates

Rates of denitrification, as determined through the production of ^{15}N-N_2, ranged from 25 to 17,053 nmol $^{15}N\ L^{-1}\ h^{-1}$ varying both with piezometer cluster and depth across the study reach (Figure 3g). We attribute this ^{15}N-N_2 production to denitrification rather than anammox as the ^{15}N-labelling of the N_2 and N_2O pools were not significantly different ($t(49)=0.766$, $p = 0.448$; Figure 4a and *see* below). The rate of denitrification generally decreased with depth in the riverbed (ANOVA, $F(4,57) = 4.0$, $p = 0.006$), except where subsurface water flux was horizontal (Table 3). The relationship between depth and denitrification was strongest within sediments with upwelling porewater (Table 3) but overall, rates of denitrification here were lowest compared to sediments with HEF or horizontal flows ($F(2,57) = 3.6$, $p = 0.034$). In the presence of HEF, there was a clear 'step down' between denitrification rates in shallow (<10cm) and deep sediments (Table 3). Rates of denitrification increased with both the DOC concentration of porewater and organic matter content of sediment (as LOI, Table 4) and when porewater chemistry was reduced (i.e. low in O_2, high Fe(II) and CH_4). We did however, observe denitrification in seemingly oxygenated sediments (*see* Supplementary Information). Even when the porewater DO concentration was > 200 μmol L^{-1} O_2 (~60% of air saturation), denitrification could still be measured at up to 3249 nmol ^{15}N–$N_2\ L^{-1}\ h^{-1}$ (median = 329 nmol ^{15}N–$N_2\ L^{-1}\ h^{-1}$, $n = 21$)

In the majority of cases, denitrification was complete, i.e. ^{15}N-N_2 comprised >99% of the ^{15}N-labelled gas produced, but there were some samples where a considerable fraction of $^{15}NO_3^-$ reduction stopped at N_2O (maximum $N_2O/N_2O + N_2 = 51\%$, median = 6%; n=9 of the 49 examined). Although the patterns were not that strong, higher values for incomplete denitrification were most strongly correlated with high Fe(II) and CH_4 i.e. where sediments were most reduced.

The denitrification rates per unit volume were integrated over the top 100 cm to give an estimate of areal activity. Areal activity ranged from 132 to 4597 μmol $^{15}N\ m^{-2}\ h^{-1}$, with a median value of 480

435 μmol ^{15}N m^{-2} h^{-1} (n=15). There was no significant difference between areal rates within different
436 hydrological settings (F(1,13) = 3.13, p = 0.01; median areal rate = 479, 562 and 1026 μmol ^{15}N m^{-2}
437 h^{-1} for strong upwelling, HEF and horizontal fluxes, respectively).
438
439 *Nitrate export using Damköhler analysis*
440 Controls on nitrate export were also investigated through calculation of Damköhler numbers, which
441 varied both with depth and piezometer cluster across the study reach (range = 0.003 to 36, n=72).
442 The majority of values however, were below the biogeochemical control threshold of Da_N=1
443 (median = 0.14, Figure 5). Da_N >1 (n=14) were generally associated with deeper sediments (e.g.
444 ≥20cm) in two piezometer clusters, sites A and G, that were characterized by HEF and horizontal
445 water fluxes, respectively.
446
447 *Nitrate attenuation in riverbed sediments*
448 Deep sediments were important sites of nitrate attenuation, however, with ~80% of denitrification,
449 on average, occurring between 10 and 100cm depth in the riverbed (Table 5, depth-integrated data).
450 On a per cm basis however, sediments within the 0-10cm depth band were sites of enhanced nitrate
451 removal under strong upwelling or HEF (Table 5, removal data per depth band divided by height of
452 depth band). Total nitrate removal per piezometer cluster was highest in sites identified as
453 biogeochemical hotspots (i.e. Da_N > 1, *see* above), similar when water flux was predominantly
454 vertical (i.e. upwelling and HEF) and lowest when water flux was horizontal (Table 5). These
455 differences however, were not statistically significant.
456
457 **4 Discussion**
458 Here, we have examined nitrate attenuation along upwelling flow pathways in a gaining reach low
459 in organic carbon, measuring nitrogen transformations *in situ*, and simultaneously characterizing
460 subsurface hydrology. Our integrated rates of denitrification (mean ± s.e. = 1078±363 μmol m^{-2} h^{-1})

461 are comparable to those measured by *in situ* "whole stream" $^{15}NO_3^-$ additions in rivers within
462 agricultural catchments [*Mulholland et al.*, 2009]. Our work adds value to the existing evidence
463 base of riverine nitrogen cycling because we also characterize denitrification below the zone of
464 surface water – groundwater mixing. Denitrification occurred throughout the 100cm depth of
465 riverbed we examined, despite the limited amount of organic carbon and the moderate O_2 content of
466 the upwelling porewater, demonstrating that the attenuation of nitrate is not just confined to shallow
467 sediments within this groundwater-fed system. Our findings are consistent with those of *Storey et*
468 *al.* [2004], *Fischer et al.* [2005] and *Stelzer et al.* [2011] and we show here that deep sediments are
469 important sites of nitrate attenuation.
470
471 **4.1 Pathways of nitrate reduction**
472 Removal of nitrate along upwelling flow pathways could occur via a number of different
473 metabolisms, e.g. denitrification, anammox and assimilatory uptake [*Burgin and Hamilton*, 2007].
474 The fate of nitrate in the riverbed is important as the benefits of nitrate attenuation could be offset if
475 the removal of nitrate occurs at the expense of production of more bioavailable and potentially
476 harmful forms of nitrogen, e.g. NH_4^+ or N_2O [*Burgin and Hamilton*, 2008; *Burgin et al.*, 2013]. In
477 agreement with our previous slurry potential incubations [*Lansdown et al.*, 2012] there was no
478 significant anammox activity *in situ* (proportion of ^{15}N in N_2 = 0.57 ≈ proportion of ^{15}N in N_2O =
479 0.54, Figure 4a) and all of the $^{15}N_2$ gas produced could be ascribed to denitrification. The decrease
480 in the proportion of ^{15}N in N_2 or N_2O relative to the injected $^{15}NO_3^-$ (98% ^{15}N) tracer, reflects
481 mixing of the tracer plume with ambient porewater $^{14}NO_3^-$ pool.
482
483 For the majority of cases, denitrification was complete, however, for a subset of samples, a
484 significant accumulation of N_2O was measured (mean ± s.d = 15±20 % N_2O, n = 9) peaking at 51%.
485 Incomplete denitrification was not restricted to individual piezometer clusters, particular hydrologic
486 settings or sediment depths. The production of N_2O in soils is well characterized but it is poorly

487 constrained in rivers; though the data available suggest a strong influence of hypoxia [*Rosamond et*
488 *al.*, 2012] and here most of the variance in the accumulation of N_2O production was correlated with
489 patches of low redox environment (accumulated NH_4^+, Fe(II) and methane) and enhanced microbial
490 activity (low O_2 saturation and fast rates of denitrification). Given N_2O has a greenhouse warming
491 potential ~280 times that of CO_2 [*Reay et al.*, 2012], the potential environmental trade-off between
492 nitrate attenuation and potent greenhouse gas production via riverbed denitrification warrants
493 further investigation.
494
495 **4.2 Interplay between hydrological and biogeochemical controls**
496 *The role of HEFs in controlling in-situ denitrification*
497 *Stelzer* and *Bartsch* [2012] described a conceptual model whereby nitrate removal within gaining
498 reaches receiving oxygenated groundwater will proceed only when the upwelling flow path
499 interacts with favorable redox conditions created through degradation of deposited and buried
500 particulate organic matter. A similar explanation was given for patterns in nitrate concentrations in
501 the River Tern, except that clay or peat lenses rather than particulate organic carbon derived from
502 ingression, controlled nitrate removal [*Krause et al.*, 2013]. Here, we have quantified denitrification
503 activity to 100cm depth in a riverbed that comprised <1% organic matter, on average (maximum
504 LOI = 3%, cf. average ~12 %, maximum = 50 % in *Stelzer* and *Bartsch* [2012]. We found no
505 evidence for lenses of buried organic matter up-gradient of the flow pathways in this reach despite
506 extensive drilling within the study site (> 100 piezometers within a 200 m reach).
507
508 It would appear that nitrate removal within this gaining reach does not require meter-scale patches
509 of buried particulate organic matter to generate favorable redox conditions for denitrification to
510 occur [sensu *Krause et al.*, 2013]. Rather, we propose that inputs of DOC and particulate organic
511 carbon to the riverbed (i) from HEF [sensu *Stelzer and Bartsch*, 2012] and (ii) via subsurface routes
512 from the floodplain or riparian zone are the key mechanisms driving heterotrophic denitrification in

513 this instance. Conceptually, HEFs could either stimulate denitrification activity by supply of labile
514 organic carbon to the sediments, or suppress denitrification activity as well oxygenated surface
515 water downwells. Here, as with our previous cm-scale investigation [*Lansdown et al.*, 2014],
516 denitrification was observed in porewaters with O_2 concentrations >200µM, although this activity is
517 probably confined to anoxic microsites within oxygenated sediments [*Triska et al.*, 1993]. The role
518 that HEFs play in increasing nitrate attenuation capacity of riverbeds [as per *Fischer et al.*, 2005;
519 *Harvey et al.*, 2013; *Zarnetske et al.*, 2011] can be observed in our shallow sediments (< 10 cm
520 depth, Table 3) around piezometer clusters A, C2 (right margin), F, H and I. In these sediments,
521 dissolved O_2 concentrations were elevated, approaching air-equilibrated values in some cases,
522 indicating ingress of well oxygenated surface water (i.e. HEFs). Supply of organic matter from the
523 river above through HEFs is inferred from elevated concentrations of DOC in porewaters at 10cm,
524 as well as accumulation of products of mineralization (ammonium, methane *see* Supplementary
525 information). Here, 44% of total depth-integrated nitrate removal (0-100 cm depth) occurred within
526 10 cm of the sediment surface highlighting the increased denitrification capacity of sediments under
527 HEFs.
528
529 It is, however, more difficult to account for the increased denitrification activity in shallow
530 sediments where strong porewater upwelling suppresses groundwater-surface water exchange (as
531 seen in chloride depth profiles of piezometer clusters B, C and D; Figure 1c). Within this
532 hydrological setting approximately 17% of total depth-integrated nitrate removal (0-100 cm depth)
533 occurred in the top 10 cm of the riverbed. Here we aimed to characterize riverbed nitrate removal
534 under base flow conditions. A parallel study at this site has quantified the effect of rising river stage
535 on porewater chemistry, finding that stage increase can cause reversal in the vertical hydraulic
536 gradient, potentially allowing surface water to infiltrate areas of the riverbed where no exchange
537 occurs under low flow conditions, altering porewater chemistry [*Byrne et al.*, 2013]. Our finding of
538 enhanced nitrate attenuation capacity within shallow sediments, with little apparent hydrological

connection to surface water, or the floodplain, could be explained by groundwater-surface water exchange or horizontal inputs under high flows (e.g. storm events) prior to the sampling campaign. The potential for such event flows to alter biogeochemical cycling, and the timescale over which processes could be affected, is poorly understood in rivers [*Zimmer and Lautz*, 2014]. Through a combination of modelling and laboratory simulation, *Gu et al.* [2008] have shown that nitrate attenuation, via denitrification in upwelling groundwater, can be altered simply through changes in residence times caused by hydraulic head variation associated with river stage rise. They did not explicitly consider what biogeochemical effects stage variation could have on the subsurface chemistry, but if a change in river stage can alter nitrate attenuation by altering residence times, even after the "event flow" has passed [*Gu et al.*, 2008], porewater chemistry and associated biogeochemical cycling (i.e. rates of denitrification) could be similarly affected.

Are hot spots of denitrification related to horizontal flow pathways?

Variation in the direction and magnitude of water fluxes alter both residence time and subsurface chemistry within the riverbed, thus affecting not only the depth distribution of biogeochemical activity, but also spatial zonation of processes such as denitrification across the riverbed. At sites A and G, the total depth-integrated rate of denitrification was two orders of magnitude higher than the rest of the reach (1259 mmol N m^{-3}). Here, porewaters were very reduced (low O_2 and high ammonium and methane), denitrification rates were very high and Damköhler numbers were >1; indicating that nitrate export is controlled by reaction-rate rather than residence time. These sites were previously identified as biogeochemical hotspots by *Heppell et al* [2013], where horizontal water fluxes (defined as lateral inputs or HEFs) dominated over groundwater upwelling, supplying organic matter to the subsurface which was then mineralized. *Heppell et al* [2013] suggested that these sites would exhibit enhanced nitrate removal, and for these patches of riverbed this is indeed the case. From more spatially extensive porewater chemistry obtained through previous work [*Heppell et al.*, 2013; *Lansdown et al.*, 2014] we estimate that such biogeochemical hotspots cover

565 approximately 2.5 % of the study reach (~47m^2) but, within which, 8% of the nitrate removal within
566 the top 1m of riverbed occurs (average removal within these biogeochemical hotspots divided by
567 average removal across the rest of the reach). These estimates of nitrate removal along horizontal
568 flow pathways were performed assuming a maximum flow path of 1m. Where flow pathways were
569 horizontal, rather than vertical, we assume that vertical and horizontal water fluxes were equal, on
570 average [see *Binley et al.*, 2013] and, therefore, that the flow pathway is approximately 45^o. As
571 such, there will be no net effect on residence time over the flow pathway if the direction of flow is
572 horizontal rather than vertical. However, this research also shows that not every area characterized
573 by horizontal flows is a hot spot of nitrate reduction. In fact, for three out of the four zones
574 associated with horizontal water movement, there was less nitrate removed from the top 100 cm of
575 sediments compared to the vertical flow settings (9 mmol N m^{-3}). The reasons for this warrant
576 further research but it is likely that variation in the origin and length of horizontal flow paths across
577 the reach will influence the quality of the DOC; for example, some horizontal pathways will
578 originate from the nearby riparian and floodplain areas potentially comprising labile DOC whilst
579 others will be from deeper groundwater and potentially be characterized by more recalcitrant DOC
580 compounds.
581
582 Through geophysical measurements *Binley et al.* [2013] also identified a preferential discharge zone
583 in this reach at sites B to D, where upwelling porewater flux was very strong and, as a result, there
584 was little exchange with surface water or horizontal water inputs. The short water residence time,
585 combined with the high nitrate load in the oxygenated upwelling porewater, led *Heppell et al.*
586 [2013] to propose that nitrate removal would be minimal within this patch of the riverbed. Our
587 results also support this finding as this preferential discharge zone is indeed a cold spot for
588 denitrification: occupying ~20% of the reach area [*Binley et al.*, 2013] but performing <2% of the
589 total denitrification that occurs within the reach (average removal from sites B, C and D divided by
590 average removal across the rest of the reach).

591

592 *The importance of deep sediments for nitrate attenuation.*

593 Across the reach as a whole, denitrification within the top 1m of the riverbed removed between 0.3
594 and 32% of nitrate exported from upwelling porewater (median = 9%) but denitrification activity
595 was not equally distributed with depth or hydrologic setting. Considering rates of denitrification
596 alone (*see* rate-determined denitrification in Table 5), as per *Stelzer et al.* [2011], deep sediments
597 (>10cm) accounted for 64% of subsurface nitrate removal. However, simply integrating
598 denitrification rates over a given depth to estimate overall nitrate removal within a volume of
599 sediments ignores the potential influence of water residence time on nitrate flux, which can be an
600 important predictor of the fate of nitrate in sediments [*Zarnetske et al.*, 2011]. Damköhler numbers
601 indicate that riverbed nitrate attenuation within this gaining reach is limited by the rate of
602 denitrification (i.e. $Da_N<1$; Figure 5) and, as a result, nitrate flux to the river above is more strongly
603 controlled by water residence time. When nitrate attenuation is considered as the interaction of
604 hydrology and biogeochemistry (i.e. the product of denitrification rate and water residence time) we
605 calculate that, on average, 81% of subsurface nitrate removal occurred within deep sediments
606 (depth-integrated denitrification in Table 5). Nitrate removal of the magnitude presented in Table 5
607 could only occur if the supply of nitrate in the upwelling porewater exceeded the removal capacity
608 of the sediments. Measured porewater nitrate concentrations compare favorably with those
609 predicted from depth-integrated nitrate loss except in the sites identified as biogeochemical hotspots
610 (Figure S2) suggesting data presented in Table 5 are likely indicative of actual rather than potential
611 nitrate removal in the sediments.

612

613 Maximum nitrate removal will occur when timescales of denitrification and water residence time
614 are well matched [*Gu et al.*, 2007] but nitrate attenuation can also be enhanced when denitrification
615 rate is fast but water residence time is short, or vice versa. *Harvey et al.* [2013] explained equal
616 contributions of fine marginal and coarse thalweg sediments to hyporheic nitrate removal via this

617 mechanism. Here we show such a relationship can also explain nitrate removal with depth in a
618 gaining reach. Where groundwater flux was predominantly vertical, (i.e. strong upwelling or HEF)
619 denitrification rates decayed with depth as the influence of the river on the sediments below
620 diminished (*see* above). Saturated hydraulic conductivity and vertical hydraulic gradients were
621 lower in deep sediments [50cm, 100cm; *Binley et al.*, 2013] resulting in longer water residence
622 times. Consequently, shallow sediments (10cm, 20cm) were characterized by fast denitrification but
623 short residence time, whilst in deep sediment denitrification was slow and residence time was long
624 in deep sediments, with a switch between the two scenarios at ~30cm (Figure 6). These results
625 illustrate that both physical and biogeochemical controls on nitrate attenuation, and the interaction
626 thereof, can vary along upwelling flow pathways in a gaining reach.
627
628 Prior use of Damköhler numbers to investigate nitrate flux within stream beds and the riparian zone
629 have assumed denitrification rate and/or water flux to be constant along flow pathways [*Gu et al.*,
630 2007; *Ocampo et al.*, 2006]. Both our study and that of *Harvey et al.* [2013] highlight the variability
631 of denitrification and water flux timescales across relatively small spatial scales (e.g. m to dm).
632 Here we have shown in a gaining reach, that denitrification is most variable within shallow
633 sediments, whilst high variation in water residence time is associated with deep sediments and,
634 therefore, use of a single denitrification rate and water flux value to categorize nitrate transport is
635 simply not appropriate.
636
637 **5. Conclusion**
638 The results of this study provide quantitative evidence for nitrate attenuation within the bed of a
639 groundwater-fed river is controlled by both biogeochemical and hydrologic processes. We have
640 shown that denitrification occurs within carbon-poor, sandy sediments to a depth of at least 1m
641 below the riverbed surface without substantial deposits of buried organic matter, at rates that are
642 generally low, but a similar order of magnitude to the global evidence base of rivers in agricultural

643 landscapes. The majority of nitrate attenuation in our reach is transport-controlled irrespective of
644 the flow pathway (vertical or horizontal). In the case of the River Leith, hyporheic exchange flows
645 and horizontal water fluxes such as shallow groundwater inputs from the floodplain or riparian zone
646 are important because they supply the precursor substrates needed to sustain denitrification. We
647 identified two hot spots of denitrification (which are reaction-rate controlled) located within areas
648 of hyporheic exchange or horizontal water flux, and we estimate that these zones account for 8% of
649 overall nitrate attenuation in the bed sediments.
650
651 Both reaction rate and water residence times change with depth in the riverbed under stable, low
652 flow conditions. Along an upwelling flow pathway residence time is the most important control on
653 nitrate removal at depth (> 20 cm) whilst the rate of denitrification increases, and leads to enhanced
654 nitrate removal near the sediment surface. Overall, our results highlight the importance of using
655 measurements of both biogeochemical reaction rates and residence time to estimate the extent of
656 nitrate removal from riverbed sediments because, in our reach, ignoring residence time
657 underestimates the importance of deep sediments for nitrate removal by about 20%.
658
659 We recommend that future work should not only continue to explore factors controlling variation in
660 transport and rate-limited reactions at the reach scale, but also to attempt to up-scale such analysis
661 to consider the effect of different hydro-geological settings on the balance of biogeochemical and
662 hydrological controls influencing nitrate removal.
663

664 **Acknowledgements**

665 This work was funded by a Natural Environment Research Council grant awarded to Lancaster
666 University (NE/F006063/1) and Queen Mary University of London (NE/F004753/1). We
667 acknowledge the Eden Rivers Trust and Lowther Estates in facilitating access to the site, the
668 Environment Agency (England & Wales) in giving consent to establishing the experimental set-up

669 in the river , and Lancaster University for installing and maintaining the physical hydrology
670 instrumentation in the river. We thank two anonymous reviewers for comments which helped
671 strengthen this paper. The data presented are available upon request from the corresponding author.

672

673 **References**

674 Addy, K., D. Q. Kellogg, A. J. Gold, P. M. Groffman, G. Ferendo, and C. Sawyer (2002), In Situ
675 Push–Pull Method to Determine Ground Water Denitrification in Riparian Zones, *J. Environ. Qual.*,
676 *31*(3), 1017-1024, doi:10.2134/jeq2002.1017.
677 Allen, D. J., J. P. Bloomfield, and V. K. Robinson (1997), The physical properties of major aquifers
678 in England and Wales, *British Geological Survey Technical Report WD/97/34*
679 312 pp, Natural Environment Research Council and Environment Agency.
680 APHA-AWWA-WPCF (1976), Standard methods for the examination of water and wastewater,
681 edited, p. 208, American Public Health Association, Washington D.C.
682 Bahr, J. M., and J. Rubin (1987), Direct comparison of kinetic and local equilibrium formulations
683 for solute transport affected by surface reactions, *Water Resour. Res.*, *23*(3), 438-452,
684 doi:10.1029/WR023i003p00438.
685 Bardini, L., F. Boano, M. B. Cardenas, R. Revelli, and L. Ridolfi (2012), Nutrient cycling in
686 bedform induced hyporheic zones, *Geochim. et Cosmochim. Acta*, *84*(0), 47-61,
687 doi:10.1016/j.gca.2012.01.025.
688 Bernot, M. L., and W. K. Dodds (2005), Nitrogen retention, removal, and saturation in lotic
689 ecosystems, *Ecosystems*, *8*, 442 - 453.
690 Binley, A., S. Ullah, A. L. Heathwaite, C. Heppell, P. Byrne, K. Lansdown, M. Trimmer, and H.
691 Zhang (2013), Revealing the spatial variability of water fluxes at the groundwater-surface water
692 interface, *Water Resour. Res.*, *49*(7), 3978-3992, doi:10.1002/wrcr.20214.
693 Burgin, A. J., and S. K. Hamilton (2007), Have we overemphasized the role of denitrification in
694 aquatic ecosystems? A review of nitrate removal pathways, *Front. Ecol. Environ*, *5*(2), 89 - 96,
695 doi:10.1890/1540-9295(2007)5[89:HWOTRO]2.0.CO;2.
696 Burgin, A. J., and S. K. Hamilton (2008), NO_3^- - driven SO_4^{2-} production in freshwater ecosystems:
697 Implications for N and S cycling, *Ecosystems*, *11*, 908 - 922.
698 Burgin, A. J., J. G. Lazar, P. M. Groffman, A. J. Gold, and D. Q. Kellogg (2013), Balancing
699 nitrogen retention ecosystem services and greenhouse gas disservices at the landscape scale, *Ecol.*
700 *Eng.*, *56*(0), 26-35, doi:10.1016/j.ecoleng.2012.05.003
701 Burt, T. P., N. J. K. Howden, F. Worrall, M. J. Whelan, and M. Bieroza (2011), Nitrate in United
702 Kingdom Rivers: Policy and Its Outcomes Since 1970, *Environ. Sci. Technol.*, *45*(1), 175-181,
703 doi:10.1021/es101395s.
704 Byrne, P., A. Binley, A. L. Heathwaite, S. Ullah, C. M. Heppell, K. Lansdown, H. Zhang, M.
705 Trimmer, and P. Keenan (2013), Control of river stage on the reactive chemistry of the hyporheic
706 zone, *Hydrol. Process.*, *28*(17), 4766 - 4779, doi:10.1002/hyp.9981.
707 Caraco, N. F., and J. J. Cole (1999), Human impact on nitrate export: An analysis using major
708 world rivers, *Ambio*, *28*(2), 167 - 170.
709 Clilverd, H., J. Jones, Jr., and K. Kielland (2008), Nitrogen retention in the hyporheic zone of a
710 glacial river in interior Alaska, *Biogeochemistry*, *88*(1), 31-46, doi:10.1007/s10533-008-9192-9.
711 Findlay, S. E. G., R. L. Sinsabough, W. V. Sobczak, and M. Hoostal (2003), Metabolic and
712 structural response of hyporheic microbial communities to variations in supply of dissolved organic
713 matter, *Limnol. Oceanogr.*, *48*(4), 1608 - 1617.

Fischer, H., F. Kloep, S. Wilzcek, and M. T. Pusch (2005), A river's liver - microbial processes within the hyporheic zone of a large lowland river, *Biogeochemistry*, *76*(2), 349-371, doi:10.1007/s10533-005-6896-y.

García-Ruiz, R., S. N. Pattinson, and B. A. Whitton (1998), Kinetic parameters of denitrification in a river continuum, *Appl. Environ. Microbiol.*, *64*(7), 2533 - 2538.

Grace, M. R., T. R. Scicluna, C. L. Vithana, P. Symes, and K. P. Lansdown (2010), Biogeochemistry and cyanobacterial blooms: investigating the relationship in a shallow, polymictic, temperate lake, *Environ. Chem.*, *7*, 443 - 456, doi:10.1071/EN10042.

Gu, C., G. M. Hornberger, J. S. Herman, and A. L. Mills (2008), Effect of freshets on the flux of groundwater nitrate through streambed sediments, *Water Resour. Res.*, *44*(5), W05415, doi:10.1029/2007WR006488.

Gu, C., G. M. Hornberger, A. L. Mills, J. S. Herman, and S. A. Flewelling (2007), Nitrate reduction in streambed sediments: Effects of flow and biogeochemical kinetics, *Water Resour. Res.*, *43*(12), W12413, doi:10.1029/2007WR006027.

Harvey, J. W., J. K. Böhlke, M. A. Voytek, D. Scott, and C. R. Tobias (2013), Hyporheic zone denitrification: Controls on effective reaction depth and contribution to whole-stream mass balance, *Water Resour. Res.*, *49*(10), 6298-6316, doi:10.1002/wrcr.20492.

Heppell, C., A. Louise Heathwaite, A. Binley, P. Byrne, S. Ullah, K. Lansdown, P. Keenan, M. Trimmer, and H. Zhang (2013), Interpreting spatial patterns in redox and coupled water–nitrogen fluxes in the streambed of a gaining river reach, *Biogeochemistry*, *117*(2-3), 491-509, doi:10.1007/s10533-013-9895-4.

Howden, N. J. K., and T. P. Burt (2008), Temporal and spatial analysis of nitrate concentrations from the Frome and Piddle catchments in Dorset (UK) for water years 1978 to 2007: Evidence for nitrate breakthrough?, *Sci. Total Environ.*, *407*(1), 507-526, doi:10.1016/j.scitotenv.2008.08.042.

Istok, J. D., M. D. Humphrey, M. H. Schroth, M. R. Hyman, and K. T. O'Reilly (1997), Single-well, "Push-Pull" test for in situ determination of microbial activities, *Ground Water*, *35*(4), 619 - 631.

Knapp, M. F. (2005), Diffuse pollution threats to groundwater: a UK water company perspective, *Q J Eng. Geol. Hydroge.*, *38*(1), 39-51, doi:10.1144/1470-9236/04-015.

Krause, S., C. Tecklenburg, M. Munz, and E. Naden (2013), Streambed nitrogen cycling beyond the hyporheic zone: Flow controls on horizontal patterns and depth distribution of nitrate and dissolved oxygen in the upwelling groundwater of a lowland river, *J Geophys. Res.-Biogeo.*, *118*(1), 54-67, doi:10.1029/2012JG002122.

Lansdown, K., C. M. Heppell, M. Dossena, S. Ullah, A. L. Heathwaite, A. Binley, H. Zhang, and M. Trimmer (2014), Fine-Scale in Situ Measurement of Riverbed Nitrate Production and Consumption in an Armored Permeable Riverbed, *Environ. Sci. Technol.*, *48*(8), 4425-4434, doi:10.1021/es4056005.

Lansdown, K., M. Trimmer, C. M. Heppell, F. Sgouridis, S. Ullah, A. L. Heathwaite, A. Binley, and H. Zhang (2012), Characterization of the key pathways of dissimilatory nitrate reduction and their response to complex organic substrates in hyporheic sediments, *Limnol. Oceanogr.*, *57*(2), 387 - 400, doi:10.4319/lo.2012.57.2.0387.

Lapworth, D. J., D. C. Gooddy, A. S. Butcher, and B. L. Morris (2008), Tracing groundwater flow and sources of organic carbon in sandstone aquifers using fluorescence properties of dissolved organic matter (DOM), *Appl. Geochem.*, *23*(12), 3384-3390, doi:http://dx.doi.org/10.1016/j.apgeochem.2008.07.011.

Laverman, A. M., C. Meile, P. Van Cappellen, and E. B. A. Wieringa (2007), Vertical Distribution of Denitrification in an Estuarine Sediment: Integrating Sediment Flowthrough Reactor Experiments and Microprofiling via Reactive Transport Modeling, *Appl. Environ. Microb.*, *73*(1), 40-47, doi:10.1128/aem.01442-06.

Maier, G., R. J. Nimmo-Smith, G. A. Glegg, A. D. Tappin, and P. J. Worsfold (2009), Estuarine eutrophication in the UK: current incidence and future trends, *Aquat. Conserv.*, *19*(1), 43-56, doi:10.1002/aqc.982.

765 Marzadri, A., D. Tonina, and A. Bellin (2011), A semianalytical three-dimensional process-based
766 model for hyporheic nitrogen dynamics in gravel bed rivers, *Water Resour. Res.*, *47*(11), W11518,
767 doi:10.1029/2011wr010583.
768 Mulholland, P. J., et al. (2009), Nitrate removal in stream ecosystems measured by N-15 addition
769 experiments: Denitrification, *Limnol. Oceanogr.*, *54*(3), 666-680, doi:10.4319/lo.2009.54.3.0666.
770 National Audit Office (2010), Tackling diffuse water pollution in England, *Report by the*
771 *Comptroller and Auditor General, Report No. HC 188 Session 2010-2011*
772 London.
773 Nielsen, L. P. (1992), Denitrification in sediment determined from nitrogen isotope pairing, *FEMS*
774 *Microbiol. Ecol.*, *86*, 357 - 362.
775 Ocampo, C. J., C. E. Oldham, and M. Sivapalan (2006), Nitrate attenuation in agricultural
776 catchments: Shifting balances between transport and reaction, *Water Resour. Res.*, *42*(1), W01408,
777 doi:10.1029/2004WR003773.
778 R Development Core Team (2012), R: A language and environment for statistical computing, edited
779 by R Foundation for Statistical Computing, Vienna, Austria.
780 Reay, D. S., E. A. Davidson, K. A. Smith, P. Smith, J. M. Melillo, F. Dentener, and P. J. Crutzen
781 (2012), Global agriculture and nitrous oxide emissions, *Nature Clim. Change*, *2*(6), 410-416,
782 doi:10.1038/nclimate1458.
783 Risgaard-Petersen, N., L. P. Nielsen, S. Rysgaard, T. Dalsgaard, and R. L. Meyer (2003),
784 Application of the isotope pairing technique in sediments where anammox and denitrification
785 coexist, *Limnol. Oceanogr.: Methods*, *1*, 63 - 73.
786 Rivett, M. O., S. R. Buss, P. Morgan, J. W. N. Smith, and C. D. Bemment (2008), Nitrate
787 attenuation in groundwater: A review of biogeochemical controlling processes, *Water Res.*, *42*,
788 4215 - 4232, doi:10.1016/j.watres.2008.07.020
789 Rosamond, M. S., S. J. Thuss, and S. L. Schiff (2012), Dependence of riverine nitrous oxide
790 emissions on dissolved oxygen levels, *Nat. Geosci.*, *5*(10), 715-718, doi:10.1038/ngeo1556.
791 Sanders, I. A., and M. Trimmer (2006), In situ application of the $^{15}NO_3^-$ isotope pairing technique
792 to measure denitrification in sediments at the surface water–groundwater interface, *Limnol.*
793 *Oceanogr.: Methods*, *4*, 142 - 152.
794 Seymour, K., J. Atkins, A. Handoo, P. Hulme, and K. Wilson (2008), Investigation into
795 groundwater-surface water interactions and the hydro-ecological implications of two groundwater
796 abstractions in the River Leith catchment, a sandstone system in the Eden Valley, Cumbria, U.K.
797 Environment Agency, Warrington.
798 Sheibley, R. W., J. H. Duff, A. P. Jackman, and F. J. Triska (2003), Inorganic nitrogen
799 transformations in the bed of the Shingobee River, Minnesota: Integrating hydrologic and biological
800 processes using sediment perfusion cores *Limnol. Oceanogr.*, *48*(3), 1129 - 1140,
801 doi:10.4319/lo.2003.48.3.1129.
802 Smart, R. M., and J. W. Barko (1985), Laboratory culture of submersed freshwater macrophytes on
803 natural sediments, *Aquat.Bot.*, *21*, 251 - 263, doi:10.1016/0304-3770(85)90053-1.
804 Smith, J. W. N. (2005), Groundwater-surface water interactions in the hyporheic zone, *Environment*
805 *Agency (UK) Science Report, Report No. SC030155/SR1*.
806 Smith, J. W. N., and D. N. Lerner (2008), Geomorphologic control on pollutant retardation at the
807 groundwater–surface water interface, *Hydrol. Processes*, *22*(24), 4679-4694, doi:10.1002/hyp.7078.
808 Stelzer, R. S., and L. A. Bartsch (2012), Nitrate removal in deep sediments of a nitrogen-rich river
809 network: A test of a conceptual model, *J. Geophys. Res.*, *117*(G2), G02027,
810 doi:10.1029/2012jg001990.
811 Stelzer, R. S., L. A. Bartsch, W. B. Richardson, and E. A. Strauss (2011), The dark side of the
812 hyporheic zone: Depth profiles of nitrogen and its processing in stream sediments, *Freshwater*
813 *Biol.*, *56*(10), 2021-2033, doi:10.1111/j.1365-2427.2011.02632.x.
814 Storey, R. G., D. D. Williams, and R. R. Fulthorpe (2004), Nitrogen processing in the hyporheic
815 zone of a pastoral stream, *Biogeochemistry*, *69*(3), 285 - 313,
816 doi:10.1023/B:BIOG.0000031049.95805.ec.

817 Thamdrup, B., and T. Dalsgaard (2000), The fate of ammonium in anoxic manganese oxide-rich
818 marine sediment, *Geochim.et Cosmochim. Acta*, *64*(24), 4157 - 4164, doi:10.1016/S0016-
819 7037(00)00496-8
820 Trimmer, M., N. Risgaard-Petersen, J. C. Nicholls, and P. Engström (2006), Direct measurement of
821 anaerobic ammonium oxidation (anammox) and denitrification in intact sediment cores, *Mar. Ecol.*
822 *Prog. Ser.*, *326*, 37-47, doi:10.3354/meps326037.
823 Triska, F. J., J. H. Duff, and R. J. Avanzino (1993), The role of water exchange between a stream
824 channel and its hyporheic zone in nitrogen cycling at the terrestrial aquatic interface,
825 *Hydrobiologia*, *251*(1-3), 167 - 184, doi:10.1007/BF00007177.
826 Zarnetske, J. P., R. Haggerty, S. Wondzell, and M. A. Baker (2011), Dynamics of nitrate production
827 and removal as a function of residence time in the hyporheic zone, *J. Geophys. Res.*, *116*, G01025,
828 doi:10.1029/2010JG001356
829 Zarnetske, J. P., R. Haggerty, S. M. Wondzell, V. A. Bokil, and R. González-Pinzón (2012),
830 Coupled transport and reaction kinetics control the nitrate source-sink function of hyporheic zones,
831 *Water Resour. Res.*, *48*(11), W11508, doi:10.1029/2012WR011894.
832 Zimmer, M. A., and L. K. Lautz (2014), Temporal and spatial response of hyporheic zone
833 geochemistry to a storm event, *Hydrol. Process.*, *28*(4), 2324-2337, doi:10.1002/hyp.9778.
834

835

List of Tables

Table 1: Summary of denitrification calculations

Parameter	Method of calculation
Rate-determined proportion[a]	$\frac{\text{Denitrification rate (nmol } {}^{15}\text{N-N}_2\ \text{L}^{-1}\ \text{h}^{-1})_{\text{depth=i}}}{\Sigma\ \text{Denitrification rate}_{\text{depth = 10,20,30,50,100cm}}}$
Depth-integrated proportion[b]	$\frac{\text{Denitrification rate (nmol } {}^{15}\text{N-N}_2\ \text{L}^{-1}\ \text{d}^{-1})_{\text{depth=i}}\ \text{x residence time (d)}_{\text{depth=i}\rightarrow\text{i'}}}{\Sigma\,\text{Denitrification rate}_{\text{depth=10,20,30,50,100cm}}\ \text{x residence time}_{\text{depth=0–10,10–20,20–30,30-50,50-100cm}}}$
Areal rate[a,b]	$\Sigma\frac{1}{2}\left[\begin{array}{l}\text{Denitrification rate } (\mu\text{mol m}^{-3}\ \text{h}^{-1})_{\text{depth=i}}\ \text{x } (\text{depth}_i - \text{depth}_{i'}\ (\text{m})) \\ +\ \text{Denit. rate}_{\text{depth=i'}}\ \text{x } (\text{depth}_i - \text{depth}_{i'})\end{array}\right]$
Damköhler number	$\text{Residence time (h)} \div \frac{1}{\frac{\text{Denit. rate (nmol } {}^{15}\text{N-N}_2\ \text{L}^{-1}\ \text{h}^{-1})}{K_m\ (\text{nM})}}$

[a]depth=i denotes any of the depths sampled (10, 20, 30, 50, 100cm) and [b] i→i' is the distance between depth = i and that sampled above (i').

Table 2: Median solute concentrations, sediment characteristics and vertical water flux by depth in the riverbed

	Water (μM)				Sediment		Vertical water flux	
Depth	NO_3^-	DOC	O_2	Cl^-	LOI (%)[a]	d_{50} (mm)[b]	(m d^{-1})	*n*=
Surface	125	187	276	701	0.9	6.5	-	7
10cm	128	170	142	433	1.1	2.2	-	15
20cm	240	166	149	408	0.8	0.62	0.12	14[c]
30cm	227	139	180	418	0.5	0.42	-	14
50cm	200	143	157	410	0.5	0.44	0.02	14[c]
100cm	303	165	197	409	0.4	0.37	0.04	15[c]

[a]LOI denotes loss on ignition, a proxy measure of organic matter within sediment. [b]d_{50} represents median grain size. [c]*n* for vertical flux measurements were 13, 14 and 14 for 20cm, 50cm and 100cm, respectively.

Table 3: Rates of denitrification measured *in situ* in the riverbed

	Denitrification (nmol $^{15}N\text{-}N_2\ L^{-1}\ h^{-1}$)				
Depth	Range	Median[a]	Upwelling[b]	Hyporheic exchange[b]	Horizontal[b]
10cm	184-6314	1081	1075	1486	1062
20cm	148-10048	539	726	531	406
30cm	47-17053	362	257	246	644
50cm	29-4165	341	221	310	666
100cm	25-2977	178	132	78	509

[a]*n* = 15 for 10 and 100cm depth bands and 14 for 20, 30 and 50cm depth bands. [b]Data are median values, *n* = 6 for all upwelling depth bands, *n* = 5 for 10, 20 and 100cm hyporheic exchange depth bands with *n* = 4 for the remaining depths in this setting, *n* = 3 for the 20cm horizontal depth band with *n* = 4 for the remaining depths in this setting.

853 Table 4: Correlation between *in situ* rates of denitrification (D15) and chemical composition of
854 porewater and sediment

	D15	O_2	NO_3^-	Fe(II)	CH_4	DOC	LOI[a]
D15	1.00						
O_2	-0.406**	1.00					
NO_3^-	-0.362**	0.547**	1.00				
Fe(II)	0.416**	-0.532**	-0.541**	1.00			
CH_4	0.394**	-0.269*	-0.442**	0.566**	1.00		
DOC	0.357*	-0.219*	-0.126	0.509**	0.297*	1.00	
LOI	0.331*	-0.343*	-0.104	-0.005	0.082	0.152	1.00

855 * $p<0.05$, **$p<0.001$. Data are spearman's rank correlation coefficients, $n = 72$ per test except [a]LOI
856 where $n = 48$.
857

858 Table 5: Comparison of nitrate removal calculated with and without inclusion of water residence
859 time in the riverbed (depth-integrated and rate-determined, respectively) and across different
860 hydrologic settings

Depth band (cm)	Proportion of Nitrate removal[a]		Nitrate removal (depth-integrated, mmol N m^{-3})[b]			
	Rate-determined	Depth-integrated	Upwelling	Hyporheic exchange	Horizontal	Hot spots[c]
0-10	0.36	0.19	2.7	7.0	1.2	24
10-20	0.28	0.12	1.8	1.1	0.5	45
20-30	0.16	0.05	1.8	0.9	1.1	24
30-50	0.12	0.25	3.5	4.2	3.8	486
50-100	0.08	0.39	6.1	2.5	5.0	687
Median per cluster removal[d]:			16	18	9	1259

861 [a]Data are average values, $n = 15$ per depth band. [b]Data are median values within each hydrological
862 setting and $n = 3$, 4 and 6 per depth band for horizontal fluxes, hyporheic exchange and upwelling,
863 respectively. [c]Sites A and G are grouped as hot spots of denitrification (*see* text). [d]Median per
864 cluster removal is the median value of the sum of all depth bands, per piezometer cluster, i.e.
865 median nitrate removal between 0 and 100cm.

Figure 1: Conceptual model of subsurface flow pathways (a), schematic of the study reach showing piezometers used in $^{15}NO_3^-$ injections (b) and depth profiles of chloride concentrations along the thalweg of the reach (c). Black circles indicate piezometers used in thalweg profiles, white circles are piezometers used for this research but not included in thalweg profiles. Each circle represents a cluster of 3 piezometers (20, 50 and 100cm).

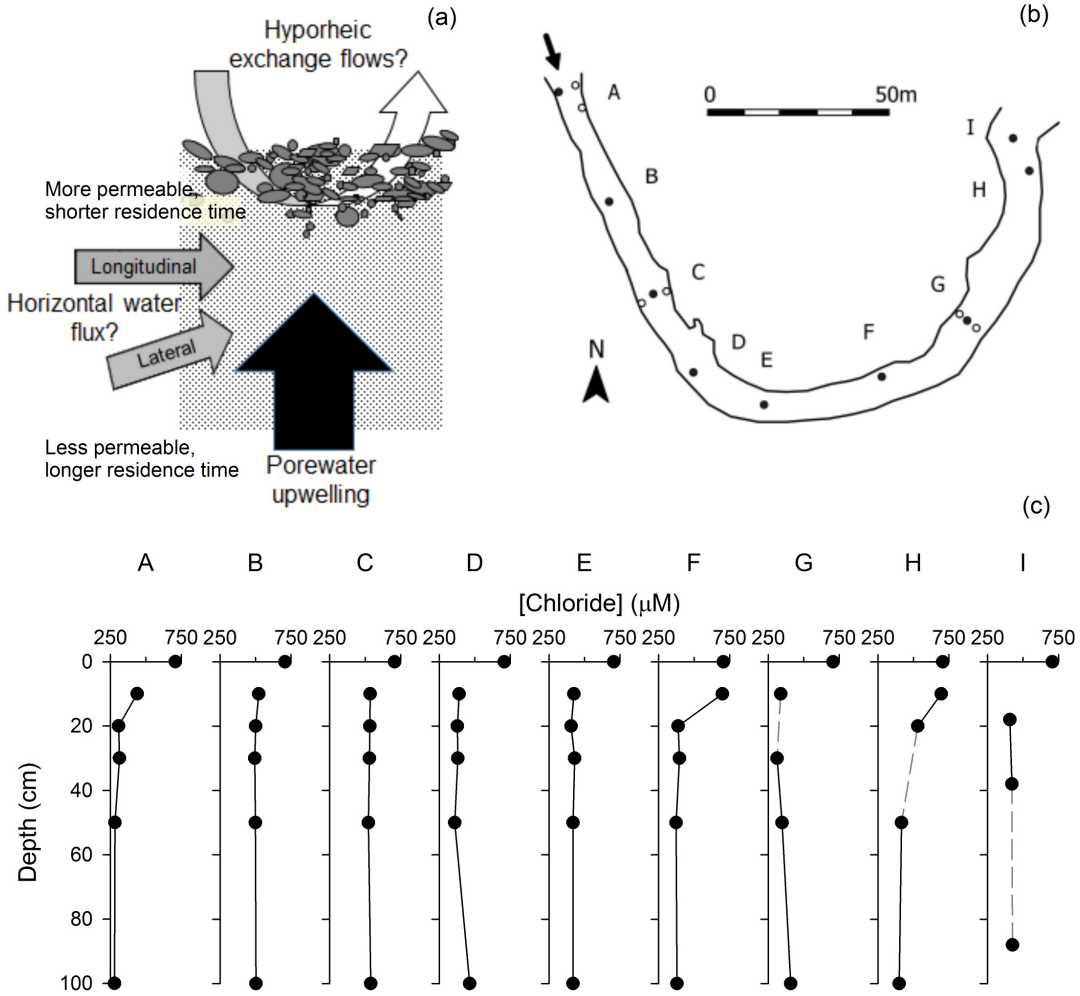

Figure 2: Characterization of subsurface hydrology using chloride concentrations in a mixing model. Mixing score is the output of a two end-member mixing model, modified such that porewater at 100cm and surface water were equal to -1 and 0, respectively. Boxes consist of median values (straight vertical line), the interquartile range (limits of the box), whiskers are the minimum and maximum values and outliers are plotted as crosses (n = 6, 5 and 4 per depth band, for (a) porewater upwelling, (b) hyporheic exchange flows (HEF) and (c) horizontal flows, respectively).

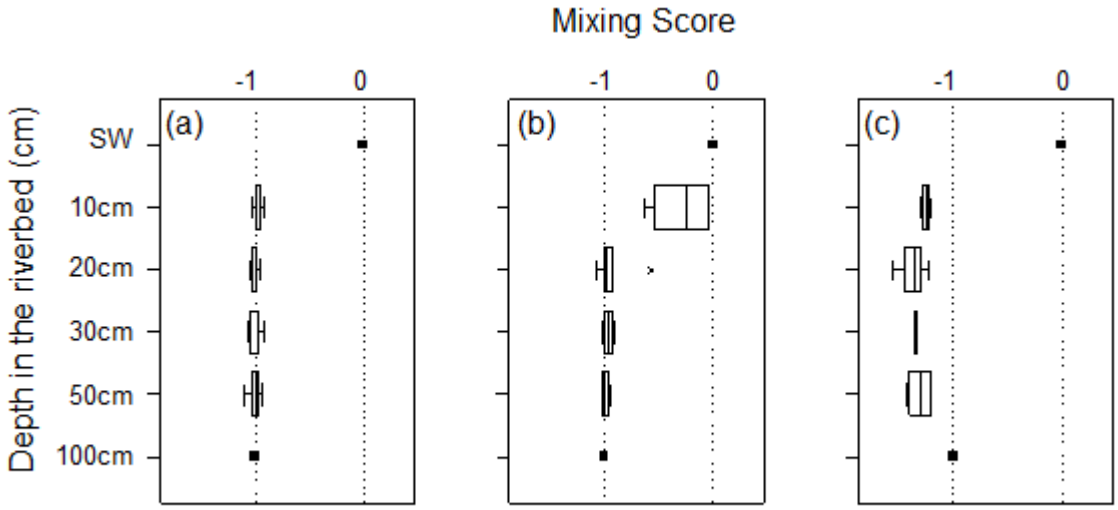

Figure 3 Spatial variation in porewater concentrations of nitrate (a,b), dissolved organic carbon (c,d), dissolved oxygen (e,f) and denitrification rate (g,h). Thalweg profiles (a,c,e,g) show individual data points from selected piezometers along the study reach (*see* Figure 1). Boxplots (b,d,f,h) contrast porewater chemistry and denitrification rate between hydrological settings with data from all piezometers. Boxes consist of median values (straight horizontal line), the interquartile range (limits of box), whiskers are the minimum and maximum values and outliers are plotted as circles.

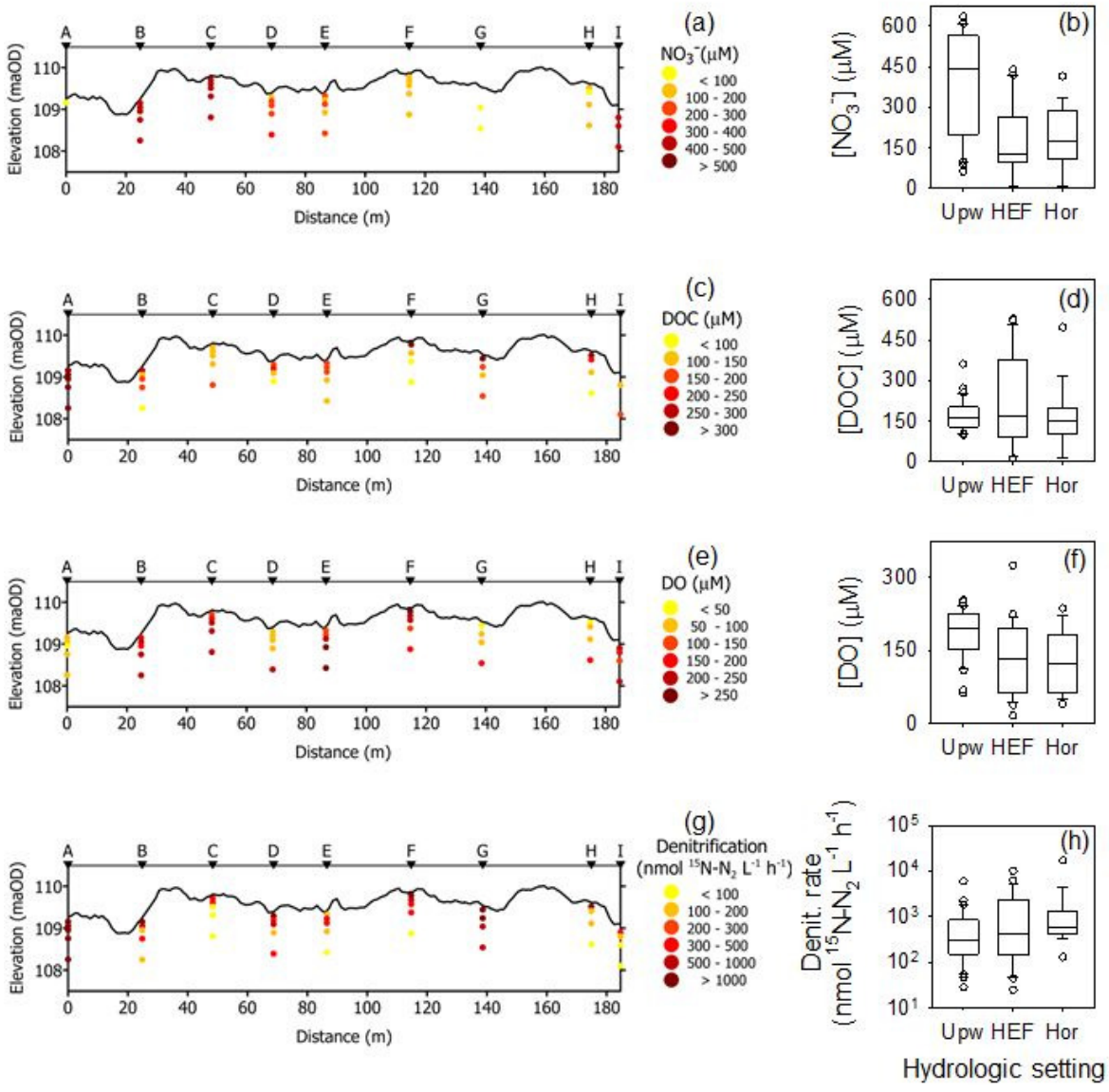

889 Figure 4: Proportion of ^{15}N labelling in the N_2 and N_2O pools (a) and proportion of ^{15}N-labelled
890 N_2O in the total nitrogenous gas pool (N_2 + N_2O, b) produced from injection of $^{15}NO_3^-$ into the river
891 bed (*n*=49 per plot). Boxplots shown in (a) consist of the median value (horizontal line),
892 interquartile range (limits of the box), the minimum and maximum values (whiskers) and outliers
893 are plotted as circles.
894

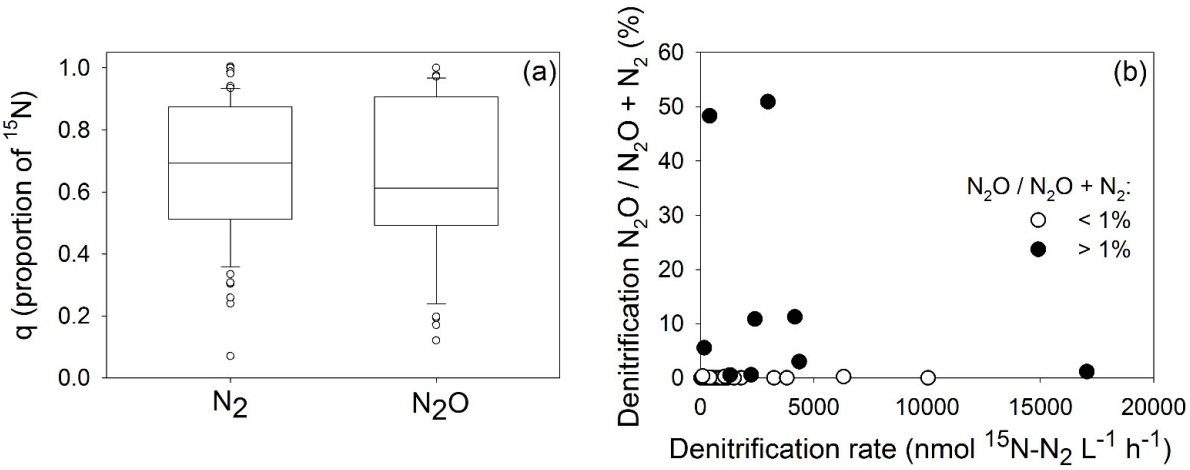

895

Figure 5: Timescales of denitrification versus timescales of water transport in a gaining reach (n=72). The solid line shows where the two timescales are equal, i.e. a Damköhler number of 1. Points that plot above the solid line represent sediments where water residence time is more important than denitrification rate in controlling nitrate flux (Da_N <1). Points that plot above the solid line represent sediments where denitrification rate is the dominant controlling factor of nitrate flux (Da_N >1).

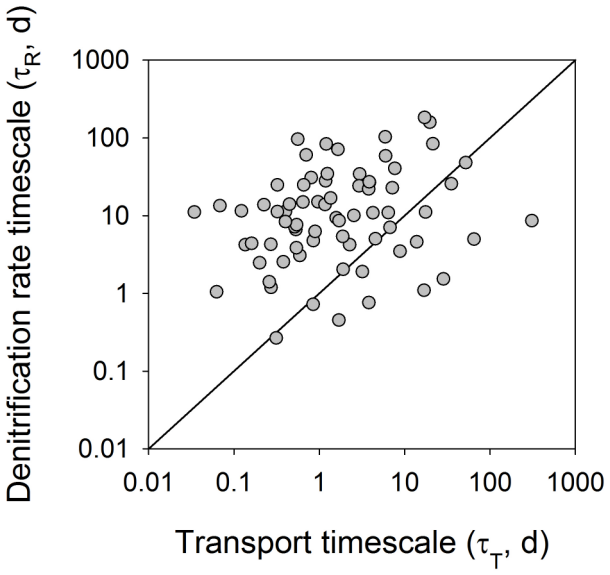

Figure 6 Variation of denitrification rate and water residence time with depth in the bed of gaining river, showing an interchange between the importance of factors controlling nitrate removal between shallow and deep sediments. Data are average values with error bars of one standard deviation.